



BATHYMETRY RETRIVEL FROM REMOTE SENSING DATA IN SHALLOW WATER OF MARSA ALAM, EGYPT

Rania Hassan*¹, Ahmed Saber², Sameh B. ElKafrawy³ and Mostafa Rabah²

¹ Department of Civil Engineering, The Technological College in Quesna, Benha, Egypt.

² Civil Engineering Department, Benha Faculty of Engineering, Benha University, Benha, Egypt.

³ Marine Sciences Department, National Authority for Remote Sensing, and Space Sciences (NARSS),
Cairo, Egypt.

ملخص البحث :

قدمت صور الأقمار الصناعية متعددة الأطياف بتقنية الاستشعار عن بعد تغطية واسعة وقلة في التكلفة وفعالية من حيث الوقت لقياس الأعماق. يتم استخدام بياناتها في عدد من التطبيقات المهمة للمناطق الساحلية الضحلة مثل المعلومات عن أعماق المياه التي تعد ضرورية لتطبيقات الهندسة الهيدرولوجية والدراسات الساحلية. تقيم هذه الدراسة أداء ثلاثة نماذج تجريبية لحسابات قياس الأعماق في جنوب مركز مرسى علم - محافظة البحر الأحمر على طريق حلايب وشلاتين. النماذج هي خوارزميات تركيب الشبكة العصبية (NN)، ودعم خوارزمية انحدار المتجهات (SVR)، وخوارزمية تركيب شجرة الانحدار باستخدام التعبئة (BAG). تم تطبيقها باستخدام صور الأقمار الصناعية سينتينال 2 لعمل خرائط الأعماق في المناطق الساحلية الضحلة باستخدام انعكاس النطاق الأخضر، الأحمر، والنسبة بين النطاقين الأزرق / الأحمر و النسبة بين النطاقين الأخضر / الأحمر. أسفرت خوارزمية (BAG) عن جذر متوسط مربع الخطأ RMSE بقيمة 0.65564م و مربع معامل الارتباط R^2 بقيمة 0.99، كما أسفرت خوارزمية (SVR) عن RMSE بقيمة 2.0474م و R^2 بقيمة 0.91 وأسفرت خوارزميات (NN) عن RMSE بقيمة 1.3430م و R^2 بقيمة 0.96. أنتجت خوارزمية (BAG) أكثر النتائج دقة ب RMSE بقيمة 0.65564م و R^2 بقيمة 0.99، مما أثبت أنها الخوارزمية المفضلة لحساب قياس الأعماق في منطقة الدراسة. الكلمات المفتاحية: خوارزميات تركيب الشبكة العصبية، وخوارزمية تركيب شجرة الانحدار باستخدام التعبئة، الأعماق، سينتينال 2، ودعم خوارزمية انحدار المتجهات.

ABSTRACT

Bathymetry measurements are important for many activities such as coastal engineering applications and hydrographical surveys. Remote sensing images provided wide coverage, low cost and time-effectiveness for bathymetry measurements. In this study data from Sentinel 2 satellite images were used to evaluate three models for bathymetry calculations in the south of MarsaAlam center - Red Sea Governorate on Halaib and Shalatin road. The models are neural network fitting algorithms (NN), support vector regression algorithms (SVR), and bagging fitting ensemble (BAG). The models used to get the depth maps in shallow coastal areas from high resolution satellite imagery using reflection of blue / red, green / red ratios, green and red bands. The BAG resulted in RMSE 0.65564m, R^2 of 0.99, the SVR yielded RMSE of 2.0474m, R^2 of 0.91 and NN yielded RMSE of 1.3430m and R^2 of 0.96 over study area. The BAG producing the most accurate results for bathymetry calculation.

KEYWORDS: Neural network, Bagging, Bathymetry, Sentinel 2, Support vector regression.

1. INTRODUCTION

Bathymetric information for shallow coastal areas is important for hydrological engineering applications as sedimentary processes, coastal studies, the purposes of monitoring underwater topography and movement of deposited sediments, and for making nautical charts in support of navigation [3]. For mapping underwater features it

is important to update the water depths information as rocks, sandy areas, sediments accumulation and coral reefs.

The conventional methods for detecting bathymetry are single multibeam echosounders or airborne LiDAR. Multibeam echosounders are considered the most accurate method, able to measure bathymetry at up to 8 cm vertical accuracy in 200 m water depth. Some equipment can detect the seabed in the depths of the water of up to 500 m with adequate vertical resolution. In contrast, Airborne LiDAR is suitable for shallow areas and can achieve vertical accuracy of up to 20 cm in water depth up to 30 meters [11,32]. But, these methods are limited by their spatial coverage, high costs, and its long time.

Estimating depth measurement using satellite imagery began in 1970 using Landsat satellite imagery [13]. After high resolution satellites were launched and is used to detect water depth, for example IKONOS [29], QUICKBIRD [5] and SPOT-4 [13]. In these previous studies, the maximum water depth at which the seafloor could be detected was 30 meters under certain conditions. In addition, the average error was about 10 cm and 30% based on water visibility, bottom type, and weather conditions [20].

Some of depth-algorithms have been developed according to the relationship between image reflection values and water depth. The first algorithm was developed by Lyzenga (1978) based on this linear relationship. This method removes the effect of the water surface and atmosphere from images, as the result the reflected values refers to the depth of the water. Limitations of this method include the assumptions that the water floor is homogeneous and that water visibility is essentially the same across the imaging area [24]. Lyzenga (1985) tried to overcome these limitations using a combination of multiple image ranges based on the multiple linear regression model of the record. Stumpf et al. (2003) improved the algorithm using the ratio between bands and correlated these values with known water depths. Indeed, the last method has no physical foundation and needs special parameters that should defined by the user [34].

Neural Network(NNs) represent an alternative algorithm suitable for depth detection. [25] began using NNs for bathymetric detection because they overcome drawbacks of conventional approaches and, in fact, possess many advantages. For example, field data requirements are reduced and NNs use raw reflection values regardless of the bottom type or water column factors. Finally, they are more practical and faster than traditional methods. NNs were also applied in other studies using various satellite images. For example, Sheela used Images of IRS P6-LISS III and Linda et al. (2011) used Quick Bird images. The limitation of their use of neural networks to detect bathymetry was that they used all image ranges as inputs to the NNs algorithm. In addition, sun luminosity and certain weather conditions may affect the estimation of water depths. This study proposed various empirical approaches for bathymetry detection in shallow coastal areas to develop an assessment and monitoring computerized system that uses the satellite images to detect bathymetry over coastal water bodies. These approaches are (NN), (SVR) and the (BAG). The proposed methodologies for detect bathymetry were applied using Sentinel 2 satellite images. The achieved results were then compared and evaluated with echosounder bathymetric data over the study areas.

2. Study areas and available data

The study area is located in the resort of Newhaven south of Marsa Alam center - Red Sea Governorate on Halaib and Shalatin road, bounded on the south by the Fantasia resort and from the West land space then Halaib road and Shalatin and from the north

by land of space then Lambrada Gamma Resort (figure 1).Newhaven Resort has a sea front on the Red Sea with a coastline of 530 meters.

The resort is characterized by a shallow area ranging from the length of the shoreline from 100 meters to 200 meters, with different benthic topography and different marine environments of marine grass and coral reefs, with the top of the reef crest (figure 2) and then the slope to deep water.

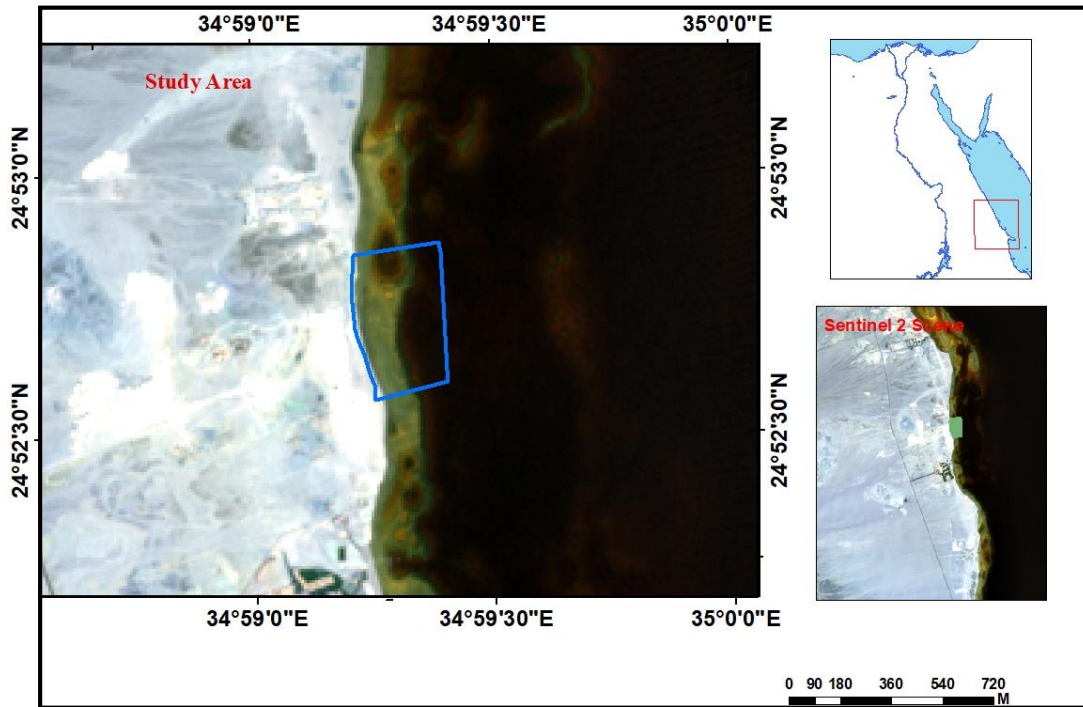


Figure 1: The study area.

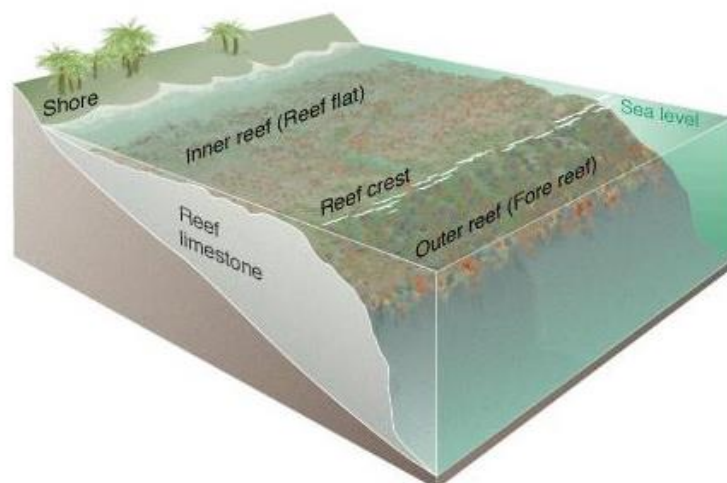


Figure 2: Section of reef crest.

2.1 Imagery data

In this research the Sentinel 2 open data satellite missions, were used. The closest time scenes at July 2018 were selected. The data of this satellite missions can be obtained from USGS Earth Explorer and Copernicus Open Access Hub.

2.2 Echosounder data

The device Bathy-500mf Multi Frequency- Survey-Echo Sounder was used on the boat to scan the longitudinal and transverse sectors of the deep area, which allows the passage of vessels without any hindrance, and the device is connected to the GPS device to determine the coordinates of each point in the sector surveyed with high accuracy. Laptop on the program of the marine hypack survey, which allows the scanner sector vision and tracking the current survey on the computer screen to ensure the direction and accuracy of scanned sectors, as well as storage and output data. In order to perform the survey with the accuracy the device was set to record readings every five seconds on Godly compound identified previously were recorded nearly 5,500 points in the deep area. The shallow area extends to about 150 meters from the shore and is difficult to reach by boat. The depth of the water is from 0 to 60 centimeter and about 5 meters to the lagoon. This is done by manual scanning device and manual GPS. The coordinates and depth of each point is recorded direct until walking in shallow water and the total points in the shallow water are about 1500 points.

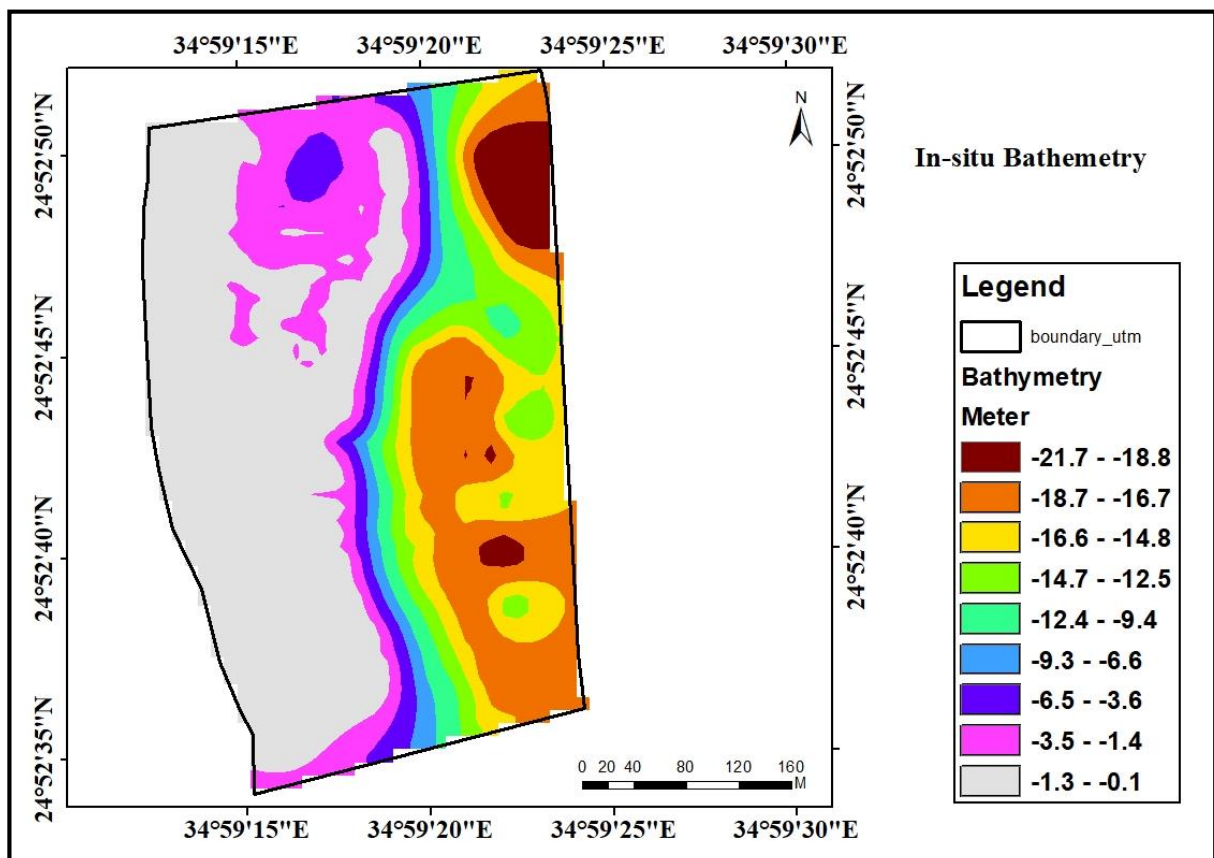


Figure 3: In-situ bathymetry.

3. Methodology

In this study, the images were acquired from Sentinel 2 satellite according to Metadata documentation; all images do not need geometric corrections. They are already in the World Geodetic System (WGS84) datum and the Universal Transverse Mercator (UTM) projection system. The Sentinel 2 multispectral images of the studied area were corrected for bathymetric mapping through three successive steps [21]. First, we converted the digital numbers of image pixels to reflectance values. Second, the image corrected for atmospheric errors. Then, the image corrected from sun glint errors. The resulting image can be linked to water depths using field calibration points. The used methodology is described as follow:

3.1 Imagery data pre-processing

The reflectance of each pixel value can be calculated using the parameters in the metadata file depended on the following equation.

$$\rho\lambda = (M_p \text{ DN} + A_p) / \sin \theta_{SE} \quad \text{Equation 1}$$

Where, $\rho\lambda$ denotes reflectance of the top of atmosphere reflectance, DN represents the digital numbers recorded by the sensor, M_p is the band-specific multiplicative rescaling factor for reflectance, A_p is the band specific additive rescaling factor for reflectance, and θ_{SE} is the local sun elevation angle in degrees. The M_p , A_p , and θ_{SE} values were obtained from the metadata file of image (MTL file).

We corrected the reflectance values for atmospheric effects using dark pixel subtraction theory. In this method no atmospheric parameters are needed and it is based on the hypothesis that the pixel with the darkest value has no reflection and the remaining value of this pixel came from the atmospheric effect. As a result, the atmospheric correction calculated by subtracting all pixels from this pixel using the following equation 2:

$$R_{ac} = R_i - R_{dp} \quad \text{Equation 2}$$

Where R_{ac} represents the corrected pixel reflectance value, R_i is the initial pixel reflectance value ($\rho\lambda$), and R_{dp} denotes the darkest pixel value.

We corrected the reflectance values for sun glint errors using the relation between the near-infrared band and other bands [9] based on the following equation:

$$R_i' = R_i * b_i (RNIR - \text{MinNIR}) \quad \text{Equation 3}$$

where R_i' denotes the de-glintoned pixel reflectance value, R_i represents the initial pixel reflectance value, b_i is the regression line slope resulting from the correlation between a sample of a visible band reflectance values and NIR band reflectance values over the glinting area, RNIR denotes the corresponding pixel value in NIR band, and MinNIR represents the minimum NIR value in the same sample of the glinting area.

4. Proposed approaches for bathymetry estimation

4.1 Neural network fitting algorithms (NN)

Neural network (NN) have been used widely in remote sensing for classification and regression problems [23]. The multilayer perception model using the back propagation algorithm is a supervised approach used for displaying the non-linear relationship

between input and output data [30]. The multilayer perception consists of: the input layers as neurons that represent the available data, which in this case is the multispectral image band values; the hidden layer that demonstrates the network training process; and finally the output layer, which are the water depths. The back propagation algorithm begins with initial network weights to find the least error values by comparing actual outputs with desired values through an iterative process eventually reaching a predefined level of accuracy [29]. Also, the linear function from the hidden layer to node outputs [3]. The Levenberg–Marquard training algorithm is used to train the back propagation for weight and bias values updating as it is the first-choice supervised algorithm that is highly recommended for training middle-sized feed-forward neural networks [28]. The algorithm is given in Equation 4 [8]:

$$X_{k+1} = X_k + [J^T J + \mu I]^{-1} J^T \epsilon_k \quad \text{Equation 4}$$

where X_k = the vector of current weights and biases, ϵ = the vector matrix of the network errors, J =Jacobian matrix of the network errors, μ = a scalar indicating the calculation speed of the Jacobean matrix, k = iteration number, I = the unit matrix, and T = the transpose matrix.

4.2 Support Vector Regression (SVR) [22]

Vapnik et al. (1964) proposed support vector machines (SVMs) for solving classification problems and statistical learning applications. As the method has shown high performance and has resulted in high accuracies, it has been extended successfully to regression problems. The support vector regression finds the most possible flat and deviated insensitive loss of function ϵ from the real targets [37]. In other words, errors are allowed if it is less than the predefined ϵ that controls the tolerance; otherwise, they are not. Suppose that we have a linear problem with the following equation:

$$F(x) = \frac{1}{4} w \cdot y + b \quad \text{Equation 5}$$

where $w \ni y$ and $b \ni y$, both w and y are the dot product of w and y , and b is the bias. Flatness in regression problems means searching for a small value for w , or in other words, minimizing the norm Euclidian space $\|w\|^2$. Thus, the regression can be stated as a convex optimisation problem as follows :

$$\begin{aligned} &\text{Minimize } \frac{1}{2} \|w\|^2 \\ &\text{Subject to} \\ &\begin{cases} t_i - (w \cdot y) + b \leq \epsilon \\ (w \cdot y) - t_i + b \leq \epsilon \end{cases} \end{aligned} \quad \text{Equation 6}$$

However, this formula assumes that all points are approximated within the allowable precision ϵ , which is not a feasible assumption in all cases, and some exceeding errors need to be allowed. A soft margin loss function is used to present slack variables ζ_i to overcome this problem, and the support vector regression solves this problem as follows: Minimize

$$\begin{aligned} &\frac{1}{2} \|w\|^2 + C \sum_{i=1}^n (\zeta_i + \zeta_i^*) \\ &\text{Subject to} \\ &\begin{cases} t_i - (w \cdot y) + b \leq \zeta_i \\ (w \cdot y) - t_i + b \leq \zeta_i^* \\ \zeta_i, \zeta_i^* \end{cases} \end{aligned} \quad \text{Equation 7}$$

Where C is the compromise between the flatness and the tolerated deviation larger than ε . The points outside ε are called support vectors.

It was found that solving this optimization problem is easier in its dual formulation and by extending the SVM to nonlinear functions. As a result, a standard idealisation method using Lagrange multipliers can be applied to solve the SVR optimization problem. A Lagrange function can be obtained from the objective function by defining a dual set of variables. The dual optimisation problem written as [9]:

Maximize

$$\begin{aligned} & -\frac{1}{2} \sum_{i,j=1}^l (\alpha_i - \alpha_j^x)(\alpha_j - \alpha_j^x)(y_i - y_j) \\ & -\varepsilon \sum_{i=1}^l (\alpha_i - \alpha_i^x) + \sum_{i=1}^l x_i (\alpha_i - \alpha_i^x) \end{aligned}$$

Subject to

$$\begin{cases} \sum_{i=1}^l (\alpha_i - \alpha_i^x) = 0 \\ (\alpha_i, \alpha_i^x) \in [0, C] \end{cases} \quad \text{Equation 8}$$

where α_i and α_i^x are Lagrange multipliers.

As a result, w and the expansion of F(x) can be calculated as follows:

$$\begin{aligned} W &= \sum_{i=1}^n (\alpha_i - \alpha_i^x) x_i \text{ and } F(x) \\ &= \sum_{i,j=1}^l (\alpha_i - \alpha_j^x)(y_i - y_j) + b \end{aligned} \quad (9)$$

The equations conclude that w can be calculated from a linear combination of the training sets of y_i .

The bias term b is calculated using the Karush Kuhn Tucker (KKT) conditions [12] as follows:

$$b = x_i - (w, y) - \varepsilon \text{ for } \alpha_i (0, C) \quad \text{Equation 10}$$

The non-linearity of the support vector algorithm can be performed by pre-processing the training sets y_i with a map $\Phi: y \rightarrow$ into some feature space.

For a practical solution, k kernel (y, y') can be used, and the support vector regression algorithm can be rewritten as follows [9]:

Maximize

$$\begin{cases} -\frac{1}{2} \sum_{i,j=1}^l (\alpha_i - \alpha_j^x)(\alpha_j - \alpha_j^x) k(y_i - y_j) \\ -\varepsilon \sum_{i=1}^l (\alpha_i + \alpha_i^x) + \sum_{i=1}^l x_i (\alpha_i - \alpha_i^x) \end{cases}$$

Subject to

$$\begin{cases} \sum_{i=1}^l (\alpha_i - \alpha_i^x) = 0 \\ (\alpha_i, \alpha_i^x) \in [0, C] \end{cases} \quad \text{Equation 11}$$

Also, w and the expression of F(x) can be rewritten as :

$$\begin{aligned} W &= \sum_{i=1}^n (\alpha_i - \alpha_i^x) \phi(x) \text{ and } F(x) \\ &= \sum_{i=1}^l (\alpha_i - \alpha_j^x) k(y_i, y_j) + b \end{aligned} \quad \text{Equation 12}$$

Next, we need the k kernel function (y, y') that corresponds to a point product in some feature space. In other words, one converts the nonlinear input space into a high

dimensional feature space. There are several kernels that can be used to perform this transformation, such as Pearson universal kernel which proposed by [36], who argued its force, the leading time-saving power leading to better circulating performance than SVRs. The global Pearson kernel can be written as follows:

$$K(y_i, y_j) = \frac{1}{1 + \frac{2 * \sqrt{\|y_i - y_j\|^2} \sqrt{2 \left(\frac{1}{\omega}\right)}}{\sigma}} \quad \text{Equation 13}$$

Where σ and ω are kernel parameters which control the half width and the tailing factor of the peak.

[26] used the sequential minimum optimisation (SMO) algorithm for solving the optimisation problem in SVR and debated its precedence to other optimisation solutions. The SMO is an iterative algorithm solving the optimisation problem analytically by breaking the optimisation problem into smaller problems. The constraints for the Lagrange multipliers are reduced as follows:

$$0 \leq \alpha_i, \alpha_i^* \leq C \text{ and } y_i \alpha_i + y_j \alpha_j^* = k$$

The algorithm starts by finding the Lagrange parameter α_i that violates the KKT conditions [12] then chooses the second Lagrange parameter α_i^* , optimizes both, and repeats these steps until convergence. When all Lagrange complications meet the conditions within the previously allowed tolerance, the problem is solved.

4.3 Bagging fitting ensemble (BAG) [21]

Breiman suggested Bag as an ensemble learning algorithm to improve prediction model performance, regression, and classification accuracy. His goal was to overcome overfitting problems and reduce algorithm variance. The objective of bagging theory is to make independent samples with replacements from the training set, and then generate a fitting model to each bootstrap sample. Finally, all generated models are aggregated by averaging in regression problems [35]. This process can be useful for improving the results of unstable algorithms as regression trees and NNs. The results are always more favourable than when using a single model [10]. The Gini diversity index can be used to split each node to assign a criterion for impurity. Splitting is finished when the Gini index reaches zero and the results are pure split nodes [25].

5. RESULTS

Figure 4 summarises the processing steps for estimating bathymetric information from Sentinel 2 satellite imagery. The first two steps involve converting the DNs to reflectance values and correcting both atmospheric and sun glint errors. These steps are performed in an ENVI environment. The proposed approaches for estimating bathymetry and all the statistical analysis are conducted in a MATLAB environment. For all proposed approaches corrected blue/red, green/red green and red bands logarithms were used as the input layer and water depths as the output layer. The data set was divided into random samples with 75% for training and 25% for testing.

The NN has been trained using Levenberg-Marquardt back-propagation training function with. The log sigmoid function was used with the hidden layer, 10 neurons were selected after many trials to get the optimum number of neurons, and the linear function with the output layer.

The SVR was applied with SMO for solving the optimisation problem and the PUK kernel function. The SVR code was originally developed [4].

The BAG model was constructed with ensembles of 30 regression trees .All of these parameters for each algorithm were selected based on the minimum RMSE and highest R^2 values.

Figures 5, 6, and 7 show the evaluation of each model, and Table 1 summarize the corresponding RMSE and R^2 values.

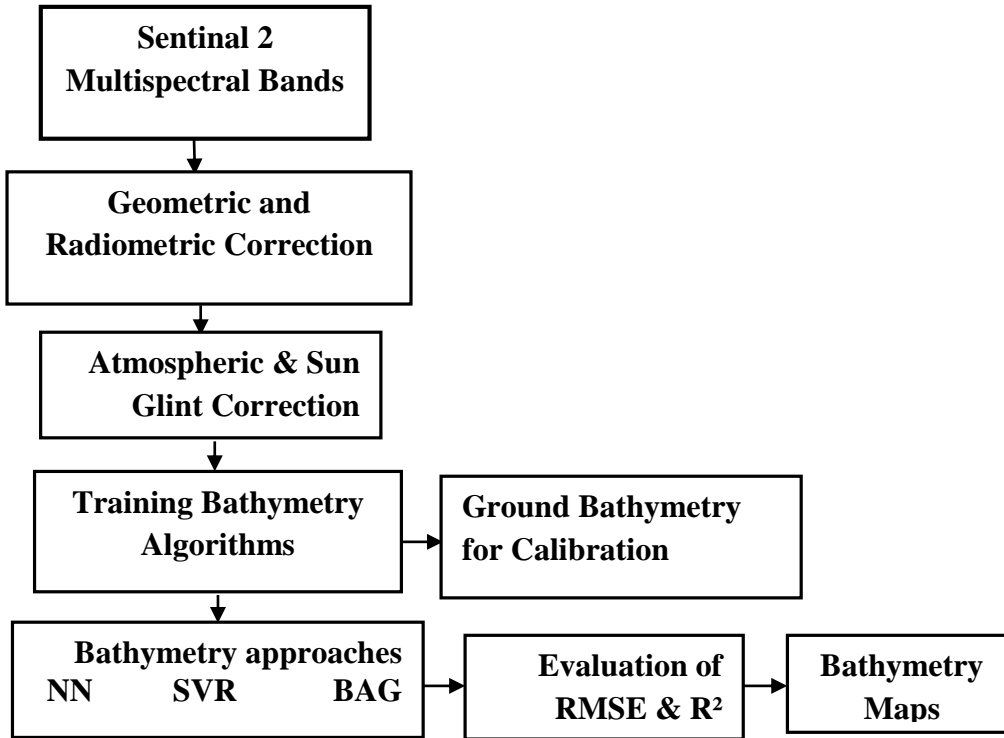


Figure 4: The workflow of the bathymetry detection steps of the study area.

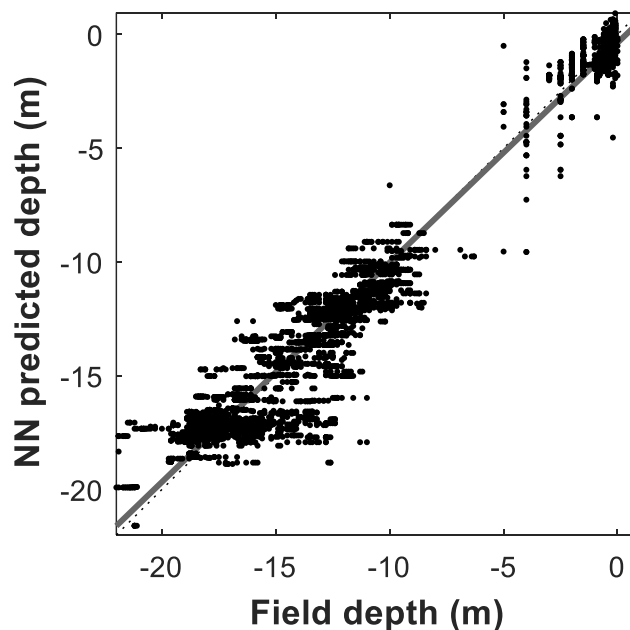


Figure 5: The continuous fitted model using NN

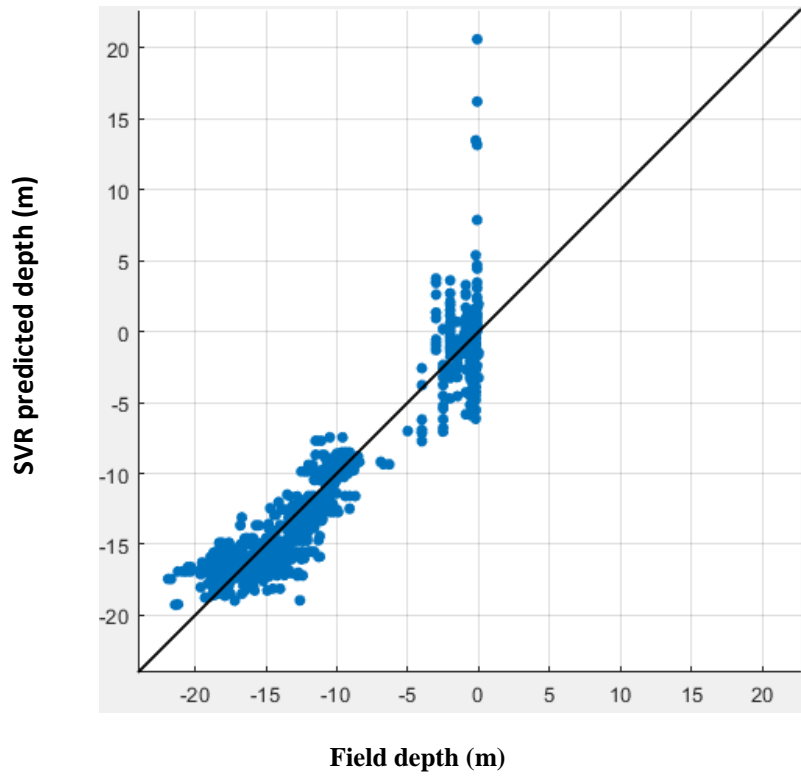


Figure 6 :The continuous fitted model using SVR

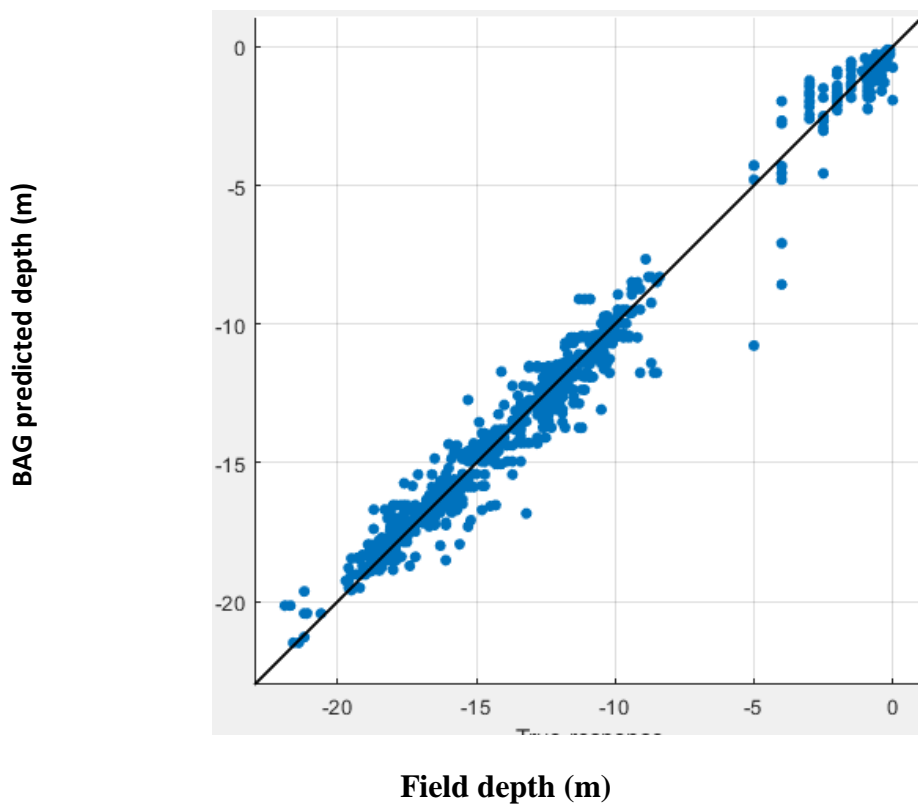


Figure 7: The continuous fitted model using BAG

Table 1: The RMSEs and R² of all methods for bathymetry detection

Methodology	NN	SVR	BAG
RMSE (m)	1.3430	2.0474	0.65564
R²	0.96	0.91	0.99

4. DISCUSSION

For bathymetry the selected bands was performed through a statistical analysis to investigate the correlation between water depth and the imagery bands. The red and green bands showed a strong relationship with the depth of the water [5,34], and as the same blue/red and green/red logarithms band ratios showed a strong relationship with the depth of the water. Finding the best combination of the selected bands is performed through a trial process based on the lowest value of RMSE and the highest value of R². At this study, the best combination occurred between the blue/red, green/red, green and red bands logarithms.

The NN performs the correlation between the multilayer of the imagery bands as input and water depth as output through multidimensional non-linear functions. Many researchers have confirmed the outperformance of NN compared to various empirical methods as it finds the highest correlation between the imagery data and the in situ water depth [7]. The main disadvantage of NN is the many experiments needed to find the best weights for the relationship as it is an unstable method that has significant differences in RMSE and R² from one experiment to another.

The SVR algorithm is as table approach that uses minimum sequential optimisation to correlate the imagery bands with water depth. The optimum kernel function was used, after many trials, from the radial basis function kernel, the polynomial kernel, and the Pearson universal kernel depended on minimum RMSE and maximum R². The latter overtook other kernel functions with the highest R² and lowest RMSE. Also, the optimum SVR parameters were selected based on the minimum RMSE criterion.

The BAG ensemble averages regression trees built from a bootstrapped random selection from input data. The optimum number of regression trees was selected after sequential trials of various numbers of trees, and the best values were achieved with 30 trees. The algorithms use the Gini diversity index for the splitting trees that are not pruned. The randomness of the regression trees and the splitting of the data into training and testing sets argue that the ensemble was not over fitting the input data.

BAG algorithm shows higher accuracies and more stability than do SVR and NN over the study area.

7. CONCLUSION

In this study three approaches were used for bathymetry detection. The proposed approaches used blue/red, and green/red, green and red bands logarithms corrected from atmospheric and sunglint systematic bands of Sentinel 2 satellite images as input data and water depth as output. To validate the proposed approaches, the approaches were compared with each other. All results were also compared with echosounder water depth data.

The proposed approaches NN, SVR and BAG, produced RMSE values of 1.3430, 2.0474 and 0.65564 m and R² values of 0.96, 0.91, 0.99 respectively.

It can be concluded that BAG approach achieved more accurate results than NN and SVR for bathymetry detection over the study area using Sentinel 2 satellite images.

REFERENCES

- [1] **Bramante JF, Raju DK, Sin TM** (2013), "Multispectral derivation of bathymetry in Singapore's shallow, turbid waters. *Int J Remote Sens*" 34(6):2070–2088. doi:10.1080/01431161.2012.734934.
- [2] **Brando V, Anstee J, Wettle M, Dekker A, Phinn S, Roelfsema C** (2009), "A physics based retrieval and quality assessment of bathymetry from suboptimal hyperspectral data". *Remote Sens Environ* 113(4):755–770. doi:10.1016/j.rse.2008.12.003.
- [3] **Ceyhun Ö, Yalçın A** (2010), "Remote sensing of water depths in shallow waters via artificial neural networks. *Estuar Coast Shelf Sci*" 89(1): 89–96. doi:10.1016/j.ecss.2010.05.015
- [4] **Clark R** (2013), "A MATLAB Implementation of Support Vector Regression (SVR)". Available on <http://www.mathworks.com/matlabcentral/fileexchange/43429-support-vector-regression>. Accessed 20 Feb 2015.
- [5] **Doxani G, Papadopoulou M, Lafazani P, Pikridas C, Tsakiri M** (2012), "Shallow-water bathymetry over variable bottom types using multispectral worldview-2 image". *ISPRS – Int Arch Photogramm, Remote Sens Spat InfSci XXXIX-B8*:159–164. doi:10.5194/isprsarchives-XXXIX-B8-159-2012.
- [6] **Farag A, Mohamed R** (2004), "Regression using support vector machines: basic foundations". Louisville University. pp. 1–17.
- [7] **Gholamalifard M, Kutser T, Esmaili A, Abkar A, Naimi B** (2013), "Remotely sensed empirical modeling of bathymetry in the southeastern Caspian Sea". *Remote Sens* 5(6):2746–2762. doi:10.3390/rs5062746.
- [8] **Hagan MT, Menhaj MB** (1994), "Training feedforward networks with the Marquardt algorithm". *IEEE Trans Neural Netw* 5(6):989–993. doi:10.1109/72.329697
- [9] Hedley JD, Harborne AR, Mumby PJ (2005), "Technical note: simple and robust removal of sunglint from aping shallow-water benthos". *Int J Remote Sens* 26(10):2107–2112. doi:10.1080/01431160500034086.
- [10] **Inoue A, Kilian L.** (2005), "How useful is bagging in forecasting economic time series? A case study of US CPI inflation". CEPR Discussion Paper No. 5304. <http://ssrn.com/abstract=872856>. Last access October 14, 2015.
- [11] **Jupp D** (1988), "Background and extension to depth of penetration (DOP) mapping in shallow coastal waters. presented at the Symposium of Remote Sensing of the Coastal Zone". Gold Coast. Queensland. IV.2.1-IV.2.19
- [12] **Karush W** (1939), "Minima of functions of several variables with inequalities asside constraints". Master thesis. Department of Mathematics, University of Chicago. USA.
- [13] **Lyzenga D.** (1981), "Remote sensing of bottom reflectance and other attenuation parameters in shallow water using aircraft and Landsat data. *International Journal of Remote Sensing* 2: 71–82. DOI: 10.1080/01431168108948342.
- [14] **Lyzenga D.** (1985), "Shallow-water bathymetry using combined Lidar and passive multispectral scanner data. *International Journal of Remote Sensing* 6: 115–125. DOI: 10.1080/01431168508948428.
- [15] **Lyzenga DR, Malinas NP, Tanis FJ** (2006), "Multispectral bathymetry using a simple physically based algorithm. *IEEE Trans Geosci Remote Sens* 44(8):2251–2259. doi:10.1109/TGRS.2006.872909.
- [16] **Leu L, Chang H.** 2005. "Remotely sensing in detecting the water depths and bed load of shallow waters and their changes. *Ocean Engineering* 32: 1174–1198. DOI: 10.1016/j.oceaneng.2004.12.005.

- [17] **Linda C, Andrea M, Marco C.** (2011), "Approaching bathymetry estimation from high resolution multispectral satellite images using a neuro-fuzzy technique. *Journal of Applied Remote Sensing* 5: 0535151–05351515. DOI: 10.1117/1.3569125.
- [18] **Loomis M.** 2009. Depth derivation from the worldview-2 satellite using hyperspectral imagery," M.S. thesis, from Naval postgraduate school Monterey, California.
- [19] **Lesser MP, Mobley CD**(2007) , "Bathymetry, water optical properties, and benthic classification of coral reefs using hyperspectral remotesensing imagery. *Coral Reefs* 26(4):819–829. doi:10.1007/s00338-0070271.
- [20] **McIntyre L, Naar F, Carder L, Donahue T, Mallinson J.** (2006)., "Coastal bathymetry from hyperspectral remote sensing data: Comparisons with high resolution multibeam bathymetry. *Marine Geophysical Researches* 27: 129–136. DOI: 10.1007/s11001-005-0266-y.
- [21] **Mohamed H, Negm A, Zahran M, and Abdel-Fattah S.** (2016)., "Estimation of Bathymetry Using High-resolution Satellite Imagery: Case Study El-Burullus Lake, Northern Nile Delta. *The Handbook of Environmental Chemistry*, Berlin, Heidelberg: Springer Berlin Heidelberg: 1–30.
- [22] **Mohamed H, Negm A, Kazuo Nadaok and Zahran M.** (2017)., "Assessment of proposed approaches for bathymetry calculations using multispectral satellite images in shallow coastal/lake areas: a comparison of five models. *Arab J Geosci*, 10: 42, DOI 10.1007/s12517-016-2803-1.
- [23] **Mather P, Tso B** (2009.) "Artificial neural networks. In *Classification Methods for Remotely Sensed Data*, Chapter 3, CRC Press. (2nd ed.), pp. 77–124. doi:10.1201/9781420090741.
- [24] **Mehdi G, Tiit K, Abbas E, Ali A, Babak N.** (2013.) "Remotely sensed empirical modeling of bathymetry in the southeastern Caspian Sea. *Remote Sensing* 5: 2746–2762. DOI: 10.3390/rs5062746.
- [25] **Ozlem A, Oguz G.** 2012. Classification of multispectral images using Random Forest algorithm. *Journal of Geodesy and Geoformation* 1: 105–112. DOI: 10.9733/jgg.241212.1.
- [26] Platt JC (1998) Fast training of support vector machines using sequential minimal optimization. *Advances in Kernel Methods* 185–208. doi: 10.1109/ISKE.2008.4731075.
- [27] **Pacheco A, Horta J, Loureiro C, Ferreira O** (2015) Retrieval of nearshore bathymetry from Landsat 8 images: a tool for coastal monitoring in shallow waters. *Remote Sens Environ* 159:102–116. doi:10.1016/j.rse.2014.12.004.
- [28] **Ranganathan A** (2004) The Levenberg-Marquardt algorithm. Honda research institute. Available on [http://twiki.cis.rit.edu/twiki/pub/Main/Advanced Dip Team B /the-levenbergmarquardt-algorithm.pdf](http://twiki.cis.rit.edu/twiki/pub/Main/Advanced%20Dip%20Team%20B/the-levenbergmarquardt-algorithm.pdf)
- [29] **Razavi BS** (2014) Predicting the trend of land use changes using artificial neural network and Markov chain model (case study: Kermanshah City). *Res J Environ Earth Sci* 6(4):215–226.
- [30] **Rumelhart DE, Hinton GE, Williams RJ** (1986) Learning internal representations by error propagation. In collection. *parallel distributed processing: explorations in the microstructure of cognition*, (Vol 1). MIT Press, Cambridge, pp 318–362.
- [31] **Stumpf R, Holderied K, Sinclair M.** 2003. Determination of water depth with high-resolution satellite imagery over variable bottom types. *Limnology and Oceanography* 48: 547–556. DOI: 10.4319/lo.2003.48.1_part_2.0547.

- [32] **Su H, Liu H, Heyman W.** 2008. Automated derivation for bathymetric information for multispectral satellite imagery using a non-linear inversion model. *Marine Geodesy* 31: 281–298. DOI: 10.1080/01490410802466652.
- [33] **Smola A, Schölkopf B** (2004) A tutorial on support vector regression. *Stat Comput* 14:199–222. doi:10.1023 /B:STCO.0000035301.49549.88.
- [34] **Sánchez-Carnero N, Ojeda J, Rodríguez D, Marquez J** (2014) Assessment of different models for bathymetry calculation using SPOT multispectral images in a high-turbidity area: the mouth of the Guadiana estuary. *Int J Remote Sens* 35(2):493–514. doi:10.1080/01431161.2013.871402.
- [35] **Shivali K, Vishakha K.** 2014. Classification of multispectral satellite images using ensemble techniques of bagging, boosting and ada-boost. *Circuits, Systems, International Conference on Communication and IT Applications (CSCITA)*, 253–258. DOI: 10.1109/CSCITA.2014.6839268.
- [36] **Üstün B, Melssen W, Buydens L** (2006) Facilitating the application of support vector regression by using a universal Pearson VII function based kernel. *ChemomIntell Lab Syst* 81(1):29–40. doi:10.1016/j.chemolab.2005.09.003.
- [37] **Vapnik V** (2000) *The nature of statistical learning theory*. Information science and statistics, 2nd edn. Springer-Verlag, New York, pp 267–290. doi:10.1007/978-1-4757-3264-1.